Available online at www.sciencedirect.com
SCIENCE DIRECT®
Bioelectrochemistry 61 (2003) 51–56
Bioelectrochemistry
www.elsevier.com/locate/bioelechem

# Studies on electrochemical properties and scavenge of superoxide anion in aprotic media by using carbon nanotubes powder microelectrode

Yingliang Wei, Xiaobo Ji, Xueping Dang, Shengshui Hu*

*Department of Chemistry, Wuhan University, Wuhan 430072, P.R. China*

Received 6 April 2003; received in revised form 19 May 2003; accepted 4 June 2003

**Abstract**

Multiwall carbon nanotubes (MWCNTs) are filled in the cavity at the tip of a microelectrode to form a carbon nanotubes powder microelectrode (CNTs-PME). CNTs-PME was used to study electrochemical properties of superoxide anion in aprotic media. The reversibility of the oxygen/superoxide anion couple ($O_2/O_2^{\cdot -}$) at the different powder microelectrode in different aprotic media was compared by cyclic voltammetry (CV). The result indicated that the nearly reversible redox process of the $O_2/O_2^{\cdot -}$ couple was obtained at a CNTs-PME. The heterogeneous electron transfer rate constant ($k_s$) can be measured by steady-state voltammogram and the result is $4.7 \times 10^{-3}$ cm $s^{-1}$, suggesting that the electrode reaction is a nearly reversible process as expected. The scavenging activities of bilirubin, α-tocopherol (vitamin E), are examined, and the experimental results confirm that α-tocopherol is the better scavenger toward $O_2^{\cdot -}$ between them.


*Keywords:* Superoxide anion; Aprotic media; Carbon nanotubes; Powder microelectrode; Scavenging activity

## 1. Introduction

Since carbon nanotubes (CNTs) was discovered by Iijima [1], it has attracted a great deal of attention for many applications such as electronic device and chemical sensors due to its nanoscale dimensions. The nanoscale dimensions and remarkable physical properties of CNTs render them unique materials with a wide range of potential applications [2]. Such potential applications would greatly benefit from the ability of CNTs to promote the electron transfer reactions of many electroactive substances when used as an electrode material in electrochemical reactions [3–5].

For our work, our interest is to develop CNTs sensors and investigate the special electrodic performance of CNTs. In order to fulfil the goals, we introduced the powder microelectrode technique. The powder microelectrode technique has been developed in Cha's et al. [6] laboratory and its basic electrochemical behavior has been reported. The remarkable advantage of the powder microelectrode (PME) is the large ''real surface area/apparent electrode area'' ratio. The apparent reversibility of redox processes can be improved obviously by using the powder microelectrode [7]. The powder microelectrode technique has been demonstrated as an ideal technique for the study of electrochemical kinetics and the detection of biomoleculars with low concentration [8–10].

Carbon nanotubes powder microelectrode (CNTs-PME) as a novel electrode, it has been used to detect nitrite and hydrazine [11,12]. Zhao et al. [13] reported the direct electrochemistry of horseradish peroxidase (HRP) at a CNTs-PME. However, on our knowledge, CNTs-PME has not been used in aprotic media. In this paper, CNTs-PME was used to study the electrochemical properties and scavenge of superoxide anion in aprotic media for the first time. The electrochemical behavior of the $O_2/O_2^{\cdot -}$ couple at a CNTs-PME was studied, which indicated that the electrode reaction was a nearly reversible redox process. A well-developed limiting current plateau for the electrochemical reduction of oxygen was obtained at a CNTs-PME. These results indicated that this novel carbon electrode has better electrodic performance for electrochemical research than conventional carbon materials. Concurrently, the scavenging activities of two kinds of antioxidants with low molecular weight were evaluated by cyclic voltammetry (CV).

* Corresponding author. Tel.: +86-27-87218904; fax: +86-27-87647617.
*E-mail address:* sshu@whu.edu.cn (S. Hu).

1567-5394/$ - see front matter © 2003 Elsevier B.V. All rights reserved.
doi:10.1016/S1567-5394(03)00059-8

## 2. Experimental

### 2.1. Reagents

Tetrabutylammonium bromide ($n$-$Bu_4NBr$), α-tocopherol, graphite powder, acetylene black powder and all the aprotic solvents including dimethylformamide (DMF), dimethylsulfoxide (DMSO) and acetonitrile (MeCN) were obtained from Shanghai Chemical Reagents, China. Bilirubin was purchased from the Sigma. Multiwall carbon nanotube (MWCNT) were from the Institute of Nanometer Materials, Huazhong Normal University, China. All the aprotic media were dried using anhydrous calcium sulfate overnight and distilled under reduced pressure. The purity of oxygen and nitrogen gases was more than 99.999%. All other reagents were of analytical reagent grade and used without further purification. $n$-$Bu_4NBr$ (0.1 M) was used as supporting electrolyte in all experimental solutions. Water used in our experiment was distilled doubly. The solutions of bilirubin and α-tocopherol were freshly prepared before the experiments.

### 2.2. Apparatus

All electrochemical experiments were performed using a 283 Potentiostat/Galvanostat (EG&G, USA) equipped with a positive feedback IR compensation circuit. A three electrode-system, including a carbon nanotubes powder microelectrode, a platinum wire counter electrode and a saturated calomel reference electrode, was employed. A salt bridge (filled with a solution of 0.1 M $n$-$Bu_4NBr$ in DMF) attached to saturated calomel electrode (SCE) was used for preventing water leakage to the cell from SCE.

### 2.3. Preparation of the CNTs-PME

The preparation method of the powder microelectrode has been reported by Cha et al. [6]. A CNTs-PME was prepared by etching the tip of a conventional Pt microdisk electrode in aqua regia so that a microcavity was formed at the tip. Then the microcavity was packed with multiwall carbon nanotube by grinding the etched tip on the surface of a carbon nanotubes-covered flat plate. Usually, the depth of the microcavity was controlled so that it was approximately equal to the diameter of the microelectrode. In this work, the diameter and depth of the microcavity of the powder microelectrode were 100 and 80 μm, respectively. The powder on the tip of CNTs-PME could be removed by sonication for about 10 min after the experiments.

### 2.4. Procedures

The current measurements were carried out by immersing the three electrodes in 10 ml DMF solution containing 0.1 M $n$-$Bu_4NBr$. The current signals were recorded using a cyclic potential scan between $-0.1$ and $-1.5$ V (vs. SCE). The reduction peak current for $O_2$ was measured at $-0.85$ V and the oxidation peak current for $O_2^{\cdot -}$ was at $-0.75$ V at a CNTs-PME in DMF. All measurements were carried out in a thermostatted cell at $(25 \pm 0.5)$ °C.

For the oxygen-saturated experiment, the solutions were bubbled with $O_2$ for at least 10 min to ensure the saturation of oxygen, and $O_2$ was continuously flowed over the solution during the experiment. For the control experiment, the solutions were deaerated by bubbling $N_2$ for at least 20 min and were protected by $N_2$ during the experiment.

## 3. Results and discussion

### 3.1. Electroreduction of oxygen to superoxide anion

#### 3.1.1. Effects of electrode materials and media

The voltammetric responses of the $O_2/O_2^{\cdot -}$ couple as a function of the electrode material were investigated for graphite powder, acetylene black powder and multiwall carbon nanotube in DMF. Fig. 1 illustrates cyclic voltammograms for the $O_2/O_2^{\cdot -}$ couple at a graphite powder microelectrode (GPME), an acetylene black powder microelectrode (AB-PME) and a CNTs-PME in DMF. The peak current at a CNTs-PME is obviously higher than that at GPME or at AB-PME. A reasonable explanation could be that the real surface area of a CNTs-PME is larger than that of a GPME or an AB-PME.

The reversibility of the $O_2/O_2^{\cdot -}$ couple was studied at three different powder microelectrodes in three aprotic media as summarized in Table 1. It can be seen from the Table 1 that the best reversibility of the $O_2/O_2^{\cdot -}$ couple is obtained in DMSO than in DMF and MeCN, which was consistent with the result reported by Sawyer et al. [14]. Compared with the conventional carbon electrode [14], the

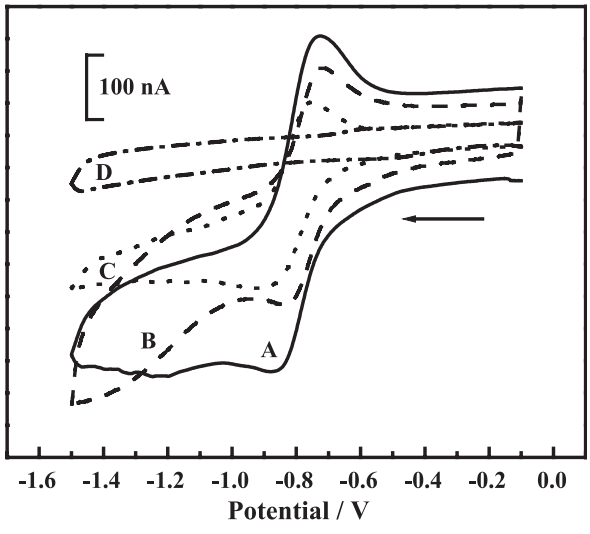


Fig. 1. Cyclic voltammograms for the $O_2/O_2^{\cdot -}$ couple at different powder microelectrode in DMF solution (air at 1 atm); scan rate: 0.1 V $s^{-1}$. A: CNTs-PME, B: AB-PME, C: GPME, D: CNTs-PME in deaerated DMF solution.

Table 1
Redox peak potentials for the $O_2/O_2^{\cdot -}$ couple by cyclic voltammetry at three different powder microelectrodes in three aprotic solvents (0.1 M *n*-$Bu_4NBr$, air at 1 atm); scan rate: 0.1 V $s^{-1}$

| Solvent | Graphite powder | | | Acetylene black | | | Multiwall carbon nanotube | | |
|---|---|---|---|---|---|---|---|---|---|
| | $E_{p,c}$ | $E_{p,a}$ | $\Delta E_p$ | $E_{p,c}$ | $E_{p,a}$ | $\Delta E_p$ | $E_{p,c}$ | $E_{p,a}$ | $\Delta E_p$ |
| DMF | −0.89 | −0.75 | 0.14 | −0.84 | −0.72 | 0.12 | −0.85 | −0.75 | 0.10 |
| DMSO | −0.81 | −0.69 | 0.12 | −0.80 | −0.70 | 0.10 | −0.80 | −0.72 | 0.08 |
| MeCN | −0.82 | −0.64 | 0.18 | −0.81 | −0.65 | 0.16 | −0.80 | −0.66 | 0.14 |

Potential ($E$): V vs. SCE, $E_{p,c}$: the cathodic peak potential, $E_{p,a}$: the anodic peak potential, $\Delta E_p$: the peak potential separation.

peak separation ($\Delta E_p$) at a CNTs-PME in DMSO decreases obviously. The results indicated that the electrode reaction was a nearly reversible redox process at a CNTs-PME in DMSO. The reason could be due to the large "real surface area/apparent electrode area" ratio of a CNTs-PME, and the apparent reversibility of redox processes can be improved obviously by using this powder microelectrode [7]. The variation of $\Delta E_p$ as the functions of electrode material and media in Table 1 could be elucidated according to heterogeneous electron transfer kinetics. Although the peak separation ($\Delta E_p$) varies with electrode material and solvent, the mean values of formal potential [$E^{\circ\prime} = (E_{p,a} + E_{p,c})/2$] are within the range between −0.73 and −0.80 V. This result is nearly consistent with the formal potential of the $O_2/O_2^{\cdot -}$ couple in aprotic media reported by Sawyer and Gibian [15].

Although the best reversibility of the $O_2/O_2^{\cdot -}$ couple at a CNTs-PME is obtained in DMSO, their redox peaks currents in DMSO are obviously lower than that in DMF due to the lower solubility of oxygen in DMSO [16]. Based on this fact, DMF was selected as the media in the following experiments.

### 3.1.2. Effect of water

It was well-known that superoxide anion reacts with water giving dioxygen and peroxide, so our experiment was performed to examine whether the small amounts of water affected the voltammetric response of the $O_2/O_2^{\cdot -}$ couple in aprotic media or not. The experimental result indicated that the modification introduced in voltammetric behavior of the $O_2/O_2^{\cdot -}$ couple was not obvious with the addition of 0.1% water in DMF. For water content of 0.2% in DMF solution, the reduction peak potential was shifted positively (0.017 V) and the oxidation peak current decreased by 9%. With the increasing amounts of water, the reduction peak potential continued to shift more positively, and the oxidation peak decreased still further. The conclusion could be drawn that a small amount of water (up to 0.1%) does not obviously affect the voltammetric response of the $O_2/O_2^{\cdot -}$ couple.

### 3.1.3. Electrochemical properties of the $O_2/O_2^{\cdot -}$ couple

The reduction peak current was measured by linear sweep voltammetry as a function of the sweep rate. It was found that the peak current increased linearly with the square root of the sweep rate up to 0.25 V $s^{-1}$, which indicated that the reduction of oxygen to superoxide anion was a diffusion-controlled process.

Fig. 2 shows typical steady-state voltammogram for the electrochemical reduction of oxygen at a CNTs-PME in oxygen-saturated DMF solution. A well-developed limiting current plateau $I_L$ can clearly be seen. The inset graph in Fig. 2 is the plot of $E$ vs. log $[(I_L - I)/I]$, and its slope ($-dE/d \log [(I_L - I)/I]$) is 0.062, suggesting that the electrochemical process of the $O_2/O_2^{\cdot -}$ couple is very close to the reversible process at the low scan rate.

The steady-state voltammogram at a microdisk electrode can be used to calculate electron transfer number ($n$) and heterogeneous electron transfer rate constant ($k_s$) [17]. For a microdisk electrode, the steady-state diffusion-controlled limiting current could be present as the generally accepted equation [17]:

$$I_L = 4nFDC^O r \quad (1)$$

where $D$ is the diffusion coefficient of oxygen in DMF, $C^O$ is the concentration of oxygen in oxygen-saturated DMF solution, $r$ is the radius of the powder microelectrode, and other symbols have their usual significance. Substituting the experimentally measured $I_L$, the value of $D$ and $C^O$ [16], and $r$ into the above equation, the electron transfer number could be calculated and the result is $n = 1.06$, indicating that the reduction of oxygen in DMF is a one-electron transfer process, i.e., oxygen is reduced to superoxide anion.

The equations reported by Glus et al. [17] for the voltammetric response of a quasi-reversible redox reaction

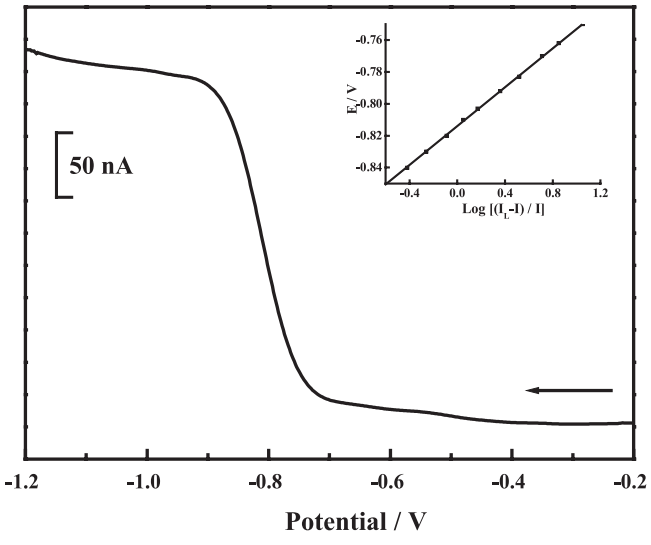


Fig. 2. Steady-state voltammogram for the electrochemical reduction of oxygen at a CNTs-PME in oxygen-saturated DMF solution; scan rate: 0.005 V $s^{-1}$; inset graph: the plot of $E$ vs. log $[(I_L - I)/I]$.

in the steady-state condition at a microdisk electrode could be depicted as follows:

$$E - E^{\circ\prime} = [(1-\alpha)nf]^{-1}\ln(4D/\pi k_s r) - [(1-\alpha)nf]^{-1}\ln[(i_l - i)/i - (i_l - i^{\tau})/i^{\tau}] \quad (2)$$

and

$$\ln[(i_l - i^{\tau})/i^{\tau}] = nf(E^{\circ\prime} - E) \quad (3)$$

where $E$ is the potential of the kinetically controlled process, $E^{\circ\prime}$ is the formal potential of the redox couple [$E^{\circ\prime}=(E_{p,a}+E_{p,c})/2$], $i^{\tau}$ is the reversible current calculated with Eq. (3) and assuming $D_o = D_R$, $i$ is the current of the kinetically controlled process measured at potential $E$, $r$ is the microdisk electrode radius, $D$ is the diffusion coefficient, $n$ is electron transfer number, $k_s$ is the heterogeneous electron transfer rate constant and $f = F/RT$, other symbols have their usual significance. Therefore, a plot of $E - E^{\circ\prime}$ vs. $\ln [(i_l - i)/i - (i_l - i^{\tau})/i^{\tau}]$ should be linear with slope $[(1-\alpha)nf]^{-1}$ and the intercept $[(1-\alpha)nf]^{-1} \ln (4D/\pi k_s r)$. If $r$ and $D$ are known, $k_s$ can be easily calculated according to the slope and the intercept of the plot. The electron transfer rate constant that was obtained in our experiment is $4.7 \times 10^{-3}$ cm $s^{-1}$, suggesting that the electrode reaction is a quasi-reversible process.

### 3.1.4. Reproducibility of the powder microelectrode

Carbon nanotubes have been confirmed to be a remarkable electrode material, which combines high stability and satisfactory reproducibility [3,4,12]. The reproducibility of a CNTs-PME was tested by consecutive cyclic potential scans. Fig. 3 illustrates cyclic voltammograms of the $O_2$/$O_2^{\cdot-}$ couple at a CNTs-PME by 10 times cyclic potential scans from $-0.1$ to $-1.5$ V. The redox peak currents keep nearly constant, indicating that the reproducibility of the CNTs-PME is satisfying.

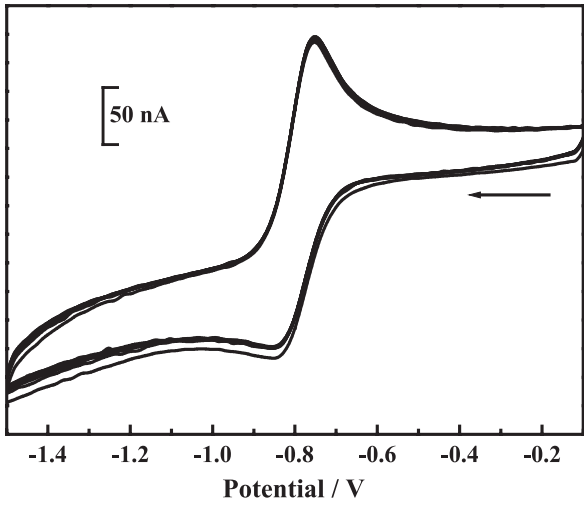


Fig. 3. Successive cyclic voltammetric responses for the $O_2/O_2^{\cdot-}$ couple at a CNTs-PME in DMF solution (air at 1 atm); scan rate: 0.05 V $s^{-1}$.

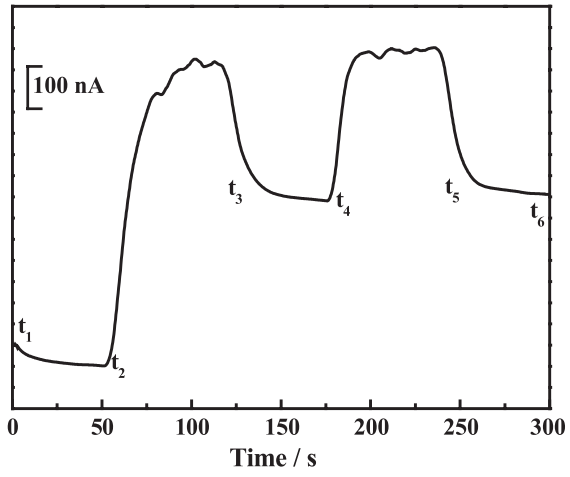


Fig. 4. Amperometric response for the reduction of $O_2$ to $O_2^{\cdot-}$ at a CNTs-PME in DMF solution; constant potential: $-1.1$ V, $t_1-t_2$, $t_3-t_4$ and $t_5-t_6$ for no bubbling $O_2$, $t_2-t_3$, $t_4-t_5$ for bubbling $O_2$.

### 3.1.5. Chronoamperometry

In order to confirming the reduction of oxygen in this system by another electrochemical method, chronoamperometry was used in our work. For amperometric measurement of the reduction of oxygen, the working electrode was operated at a constant potential of $-1.1$ V. Fig. 4 shows the amperometric response of the reduction of oxygen. The solution is air-saturated in $t_1-t_2$, and the solution is bubbled with $O_2$ in $t_2-t_3$. The reduction peak current increases dramatically during bubbling $O_2$ ($t_2-t_3$), the reason is likely that the solution is flowing and reactant ($O_2$) reaches the surface of working electrode rapidly. Although the solution is not bubbled with $O_2$ in $t_3-t_4$, the current plateau in $t_3-t_4$ is obviously higher than that in $t_1-t_2$ since the content of $O_2$

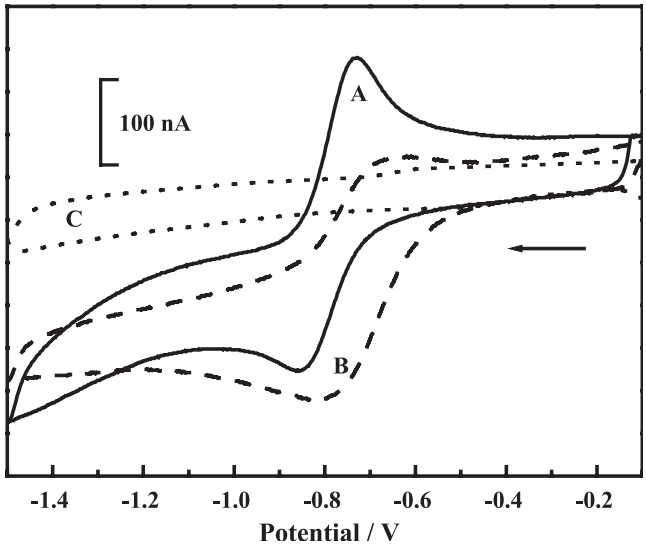


Fig. 5. Cyclic voltammograms for the scavenge of $O_2^{\cdot-}$ with bilirubin in DMF solution, scan rate: 0.1 V $s^{-1}$. A: DMF solution (air at 1 atm), B: A + 4 mM bilirubin, C: 4 mM bilirubin in deaerated DMF solution.

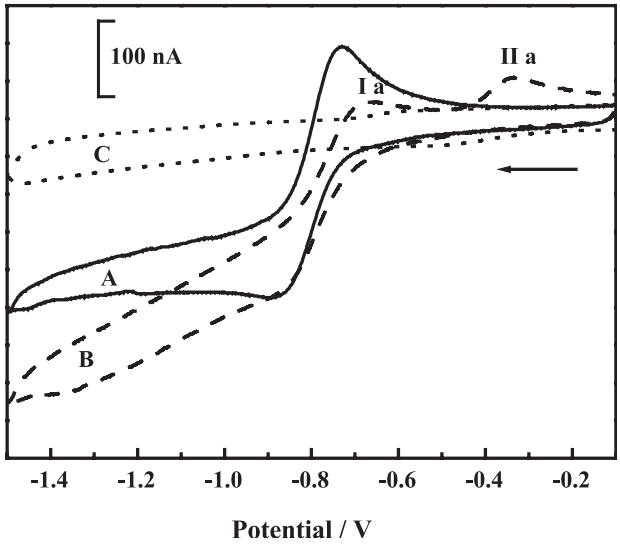


Fig. 6. Cyclic voltammograms for the scavenge of $O_2^{\cdot -}$ with α-tocopherol in DMF solution; scan rate: 0.1 V $s^{-1}$. A: DMF solution (air at 1 atm), B: A + 2 mM α-tocopherol, C: 2 mM α-tocopherol in deaerated DMF solution.

in DMF solution in $t_3-t_4$ is higher than that in $t_1-t_2$. After another period of bubbling $O_2$ ($t_4-t_5$), one appreciably higher current plateau than that in $t_3-t_4$ can be seen in $t_5-t_6$. The experimental result indicates that the reduction current increases with increasing the content of $O_2$.

### 3.2. Scavenge of superoxide anion

The investigation on scavenge of superoxide anion will be useful in understanding the protection of biological systems against reactive oxygen species (ROS). α-Tocopherol (vitamin E), bilirubin, are the excellent free radical scavengers [18–20]; they can react with many reactive species generated in the biological milieu. Although much is known about their scavenging activities for $O_2^{\cdot -}$ in biological system, the comparison concerning their scavenging ability to $O_2^{\cdot -}$ by electrochemical methods was seldom found. Here, the scavenging abilities of these liposoluble antioxidants in aprotic media were evaluated in order to do some preparatory work for study on their scavenging abilities in the biological system by ultramicrosensor.

In order to evaluate scavenging activities of bilirubin and α-tocopherol in this system, voltammetric procedures were performed. Fig. 5 illustrates cyclic voltammograms for the scavenges of $O_2^{\cdot -}$ with bilirubin in DMF. When the content of bilirubin is up to 0.3 mM, the oxidation peak current for $O_2^{\cdot -}$ does not decrease. With increasing its concentration, the oxidation peak current decreases gradually. The scavenging activity of the antioxidant is often evaluated according to its $IC_{50}$, which is defined by the concentration inhibiting the reaction by 50%. In this system, $IC_{50}$ of bilirubin is 3.5 mM. Fig. 6 shows cyclic voltammograms of 2 mM α-tocopherol in DMF solution and deaerated DMF solution. It can be seen from Fig. 6 that the oxidation peak current decreases obviously with addition of α-tocopherol. The oxidation peak ($II_a$) in Fig. 6 may arise from the intermediate product instead of α-tocopherol. In this work, $IC_{50}$ of α-tocopherol is 1.8 mM. From our experiments, the result indicated that the scavenging ability of α-tocopherol is stronger than bilirubin.

The reaction mechanism of α-tocopherol with $O_2^{\cdot -}$ has been proposed by Afanas'ev et al. [21]. Although α-tocopherol is good radical scavenger, superoxide anion is not able to abstract a hydrogen atom from them. The reaction of α-tocopherol with $O_2^{\cdot -}$ undergo a deprotonation mechanism to form corresponding anion. The reaction mechanism of α-tocopherol with $O_2^{\cdot -}$ was depicted as follows:

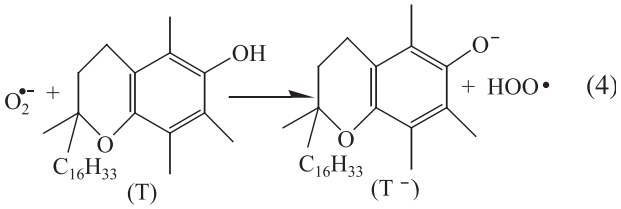


(4)

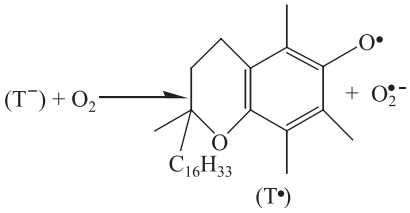


(5)

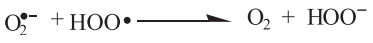


(6)

## Acknowledgements

This research was supported by grants from the National Natural Science Foundation of China (No. 60171023).

## References

[1] S. Iijima, Helical microtubules of graphitic carbon, Nature 354 (1991) 56–58.
[2] P.M. Ajayan, O.Z. Zhou, Carbon nanotubes, Top. Appl. Phys. 80 (2001) 391–425.
[3] P.J. Britto, K.S.V. Santhanam, P.M. Ajayan, Carbon nanotube electrode for oxidation of dopamine, Bioelectrochem. Bioenerg. 41 (1996) 121–125.
[4] J.J. Davis, R.J. Coles, H.A.O. Hill, Protein electrochemistry at carbon nanotube electrodes, J. Electroanal. Chem. 440 (1997) 279–282.
[5] P.J. Britto, K.S.V. Santhanam, A. Rubio, J.A. Alonso, P.M. Ajayan, Improved charge transfer at carbon nanotube electrodes, Adv. Mater. 11 (1999) 107–154.
[6] C.S. Cha, C.M. Li, H.X. Yang, P.F. Liu, Powder microelectrodes, J. Electroanal. Chem. 368 (1994) 47–54.

[7] J. Chen, C.S. Cha, Detection of dopamine in the presence of a large excess of ascorbic acid by using the powder microelectrode technique, J. Electroanal. Chem. 463 (1999) 93–99.
[8] L. Xiao, J. Chen, C.S. Cha, Elimination of the interference of ascorbic acid in the amperometric detection of biomolecules in body fluid samples and the simple detection of uric acid in human serum and urine by using the powder microelectrode technique, J. Electroanal. Chem. 495 (2000) 27–35.
[9] P.F. Liu, J.T. Lu, J.W. Yan, Nitrite reduction at powder microelectrodes, J. Electroanal. Chem. 469 (1999) 196–200.
[10] W.Y. Tu, W.J. Liu, C.S. Cha, B.L. Wu, Study of the powder/membrane interface by using the powder microelectrode technique: I. The Pt-black/Nafion interfaces, Electrochim. Acta 43 (1998) 3731–3739.
[11] P.F. Liu, J.H. Hu, Carbon nanotube powder microelectrodes for nitrite detection, Sens. Actuators, B 84 (2002) 194–199.
[12] Y.D. Zhao, W.D. Zhang, H. Chen, Q.M. Luo, Anodic oxidation of hydrazine at carbon nanotube powder microelectrode and its detection, Talanta 58 (2002) 529–534.
[13] Y.D. Zhao, W.D. Zhang, H. Chen, Q.M. Luo, S.F.Y. Li, Direct electrochemistry of horseradish peroxidase at carbon nanotube powder microelectrode, Sens. Actuators, B 87 (2002) 168–172.
[14] D.T. Sawyer, G. Chlercalo Jr., C.T. Angells, E.J. Nanni Jr., T. Tsuchlya, Effects of media and electrode materials on the electrochemical reduction of dioxygen, Anal. Chem. 54 (1982) 1720–1724.
[15] D.T. Sawyer, M.J. Gibian, The chemistry of superoxide ion, Tetrahedron 35 (1979) 1471–1481.
[16] M. Tsushima, K. Tokuda, T. Ohsaka, Use of Hydrodynamic chronocoulometry for simultaneous determination of diffusion coefficients and concentrations of dioxygen in various media, Anal. Chem. 66 (1994) 4551–4556.
[17] Z. Glus, J. Golas, J. Osteryoung, Determination of kinetic parameters from steady-state microdisk voltammograms, J. Phys. Chem. 92 (1988) 1103–1107.
[18] L.M. McCune, T. Johns, Antioxidant activity in medicinal plants associated with the symptoms of diabetes mellitus used by the Indigenous Peoples of the North American boreal forest, J. Ethnopharmacol. 82 (2002) 197–205.
[19] J.M. May, How does ascorbic acid prevent endothelial dysfunction? Free Radic. Biol. Med. 28 (2000) 1421–1429.
[20] M.-F. Chen, L.-R. Mo, R.-C. Lin, J.-Y. Kuo, K.-K. Chang, C. Liao, Increase of resting levels of superoxide anion in the whole blood of patients with decompensated liver cirrhosis, Free Radic. Biol. Med. 23 (1997) 672–679.
[21] I.B. Afanas'ev, V.V. Grabovaetskii, N.S. Kuprianova, Kinetics and mechanism of the reactions of superoxide ion in solution: Part 5. Kinetics and mechanism of the interaction of superoxide ion with vitamin E and ascorbic acid, J. Chem. Soc., Perkin Trans. II (1987) 281–285.